

RESEARCH ARTICLE

Applying the first principle to study the structure, electrical and magnetic properties of ASiNRs-doped Neodymium

Thanh Tung Nguyen^{1,*}, Thanh Xuan²

¹ Institute of Southeast Vietnamese Studies, Thu Dau Mot University, Vietnam

² Science Office, Thu Dau Mot University, Vietnam

* Corresponding author: Thanh Tung Nguyen, nttung@tdmu.edu.vn

ABSTRACT

In this project, we investigated and investigated the optimal sites in the chemisorption of Neodymium (Nd) on armchair silicene nanoribbons (ASiNRs) to learn about the geometrical and electronic properties of the structures by applying these properties with first principle math. The survey has three steps. The first was to change the top, valley, bridge, and hollow positions to find optimized position. The results show that the Bridge position has the lowest absorbed energy value of -2.6eV, has the most stable structure, with the strongest magnetic moment of 4.68 μ B, and a buckl degree of 0.69 Å; The Si-Si-Si bond angle at this time is 115.053° almost like the pristine case. The second was to change the Si-Si bondlength of ASiNRs the same purpose. Finally, we survey the distance from Nd atom to pristine adsorbent surface was decreased. The calculation results show that the valley position is the most ideal location, corresponding to the bond length of 2.26 Å and the optimal height of 2.11 Å resulting in a single material adsorption system for the new materials, different from other positions with bandgap changed. This result shows that the absorption method between metals and pristine semiconductor ASiNRs has opened up a very good direction, contributing to enriching the source of materials applied to the field of manufacturing electronic, optoelectronic, and spintronic components in the future.

Keywords: Nd adsorption SiNRs; spintronic material; optoelectronic material

1. Introduction

Silicon (Si) is an element of group IV, possessing a single electron configuration can exist in many different allotropic forms under many different sizes^[1]. Similar to the development of carbon (C)-based materials, cubic allotropes. The 3D, one-dimensional (1D)^[2], and zero-dimensional (0D) of Si were soon discovered, in which the traditional 3D cubic structure of silicon is known as the main component in semiconductor devices. Low-dimensional Si conformations such as 1D nanotubes and 0D fullerenes were also discovered very early, while the basic 2D structure of Si was predicted only in 1994^[3]. This 2D Si structure has only attracted much attention since the first successful synthesis of 2D graphene in 2004^[4].

ARTICLE INFO

Received: 21 April 2024 | Accepted: 26 June 2024 | Available online: 3 July 2024

CITATION

Nguyen TT, Xuan T. Applying the first principle to study the structure, electrical and magnetic properties of ASiNRs-doped Neodymium. *Micromaterials and Interfaces* 2024; 2(1): 6308. doi: 10.59429/mi.v2i1.6308

COPYRIGHT

Copyright © 2024 by author(s). *Micromaterials and Interfaces* is published by Arts and Science Press Pte. Ltd. This is an Open Access article distributed under the terms of the Creative Commons Attribution License (<https://creativecommons.org/licenses/by/4.0/>), permitting distribution and reproduction in any medium, provided the original work is cited.

This 2D Si structure is called silicene and is known as the closest clone of graphene materials^[5]. Silicene has a low bumpy hexagonal lattice structure with sp^2 hybrid orbital hybridization sp^2/sp^3 in Si-Si bonds^[6]. Orbital hybridization mechanism sp^2 mixture This sp^2/sp^3 indicates that the cleavage of π and σ bonds in silicene is similar relatively weak compared to sp^2 hybridization of graphene although both silicene and graphene have the Dirac cone structure is made up of p_z orbitals in the low energy^[7]. Experimentally, silicene can only be synthesized through the method raise epitaxy from the bottom up (bottom-up) because element Si does not exist in layered structure in natural as graphite^[8].

Silicon possesses many potential new physical properties for many applications such as active silicene-based field-effect transistors (FETs) room temperature sensors^[9], 2D sensors^[10], and energy storage devices^[11]. Besides, many other solid physical properties of silicene have also been discovered including large bandgap caused by spin-orbit capture at the Dirac point^[12], the effect of large quantum spin Hall^[13], transition from topologically insulating phase to insulating phase region. Potential new physical properties of silicene suggest that silicene can is a promising 2D candidate to replace graphene not only because of its 2D material similar to graphene but also better compatibility with electronic devices based on Si. However, silicene's small band gap limits its potential in nanoelectronics applications^[14].

Therefore, extending the bandgap for silicene has become a fascinating research topic that has received much attention recently. A lot of different methods have been used to generate bandgap in silicone consisting of finite-size confinement of 2D, atom-doped silicene nanosheets^[15], surface functionalization^[16], different layered structures^[17], mechanical strain^[18], and applying external fields^[19]; where chemical change is one of the methods effective methods to enrich the essential properties of silicene.

Using calculations in the original principle, the adsorption of hydrogen and halogen atoms on silicene was researched. In addition, halogenated silicene materials have been demonstrated by low-temperature tunneling microscopy (STM) studies^[20]. Structures 2D silicene has low warping when adsorbing atoms, it becomes a 2D structure with high the higher warping is due to the large deformation of the π bonds and the weakening of the σ bonds. In terms of geometry, the simplest and most effective method to open the forbidden zone of the energy for silicene is to induce finite-size confinement of 2D silicene. The quantum confinement of 2D silicene will form 1D silicene bands (SiNRs)^[21]. Finite-size confinement of the 2D silicene structure produces 1D silicene bands with two typical edge structures are armchair (ASiNR) and zigzag (ZSiNR)^[22, 23]. From the point of view of change chemically, atomic doping is an effective method for drastically altering the properties of essentiality of 1D SiNRs. This doping method can cause strong diversity in different concentrations and atomic distributions. To date, many other types of atoms each other been used for doping in SiNRs 1D. Cu atom adsorption on ZSiNR 1D has been studied by first-principle calculations. The results of this study showed that the charge transfer from the Si atom to the Cu atom leads to the state ferromagnetic^[24]. In addition, the adsorption effect of Ti atom on 1D ZSiNR has also been found studied, in which Ti atoms adsorb optimally at the hole position near the center of the band 1D^[25].

In this project, we learn about Nd (Neodymium) materials and do Nd doping into ASiNRs substrates with chemisorption. Neodymium is a chemical element with the symbol Nd and atomic number 60. It is a hard, slightly malleable, silvery metal that quickly tarnishes in air and moisture. When oxidized, neodymium reacts quickly producing pink, purple/blue and yellow compounds in the Nd⁺², Nd⁺³ and Nd⁺⁴ oxidation states [26]. Metallic neodymium has a bright, silvery metallic luster[27]. Neodymium commonly exists in two allotropic forms, with a transformation from a double hexagonal to a body-centered cubic structure taking place at about 863°C[28]. Neodymium, like most of the lanthanides, is paramagnetic at room temperature and becomes an antiferromagnet upon cooling to 20 K (−253.2°C)[29]. Neodymium is a rare-earth metal that was present in the classical mischmetal at a concentration of about 18%. To make neodymium magnets it is alloyed with iron, which is a ferromagnet[30]. In the periodic table, it appears between the lanthanides praseodymium to its left and the radioactive element promethium to its right, and above the actinide uranium. Its 60 electrons are arranged in the configuration [Xe]4f⁴6s², of which the six 4f and 6s electrons are valence. Like most other metals in the lanthanide series, neodymium usually only uses three electrons as valence electrons, as afterwards the remaining 4f electrons are strongly bound: this is because the 4f orbitals penetrate the most through the inert xenon core of electrons to the nucleus, followed by 5d and 6s, and this increases with higher ionic charge. Neodymium can still lose a fourth electron because it comes early in the lanthanides, where the nuclear charge is still low enough and the 4f subshell energy high enough to allow the removal of further valence electrons[31]. The experimental study designed to explore the electrical properties at the Nd-doped Si-SiO₂ interface. The Nd-doped silicon wafers and control silicon wafers (undoped) were annealed under different conditions of temperature, time and atmosphere [32].

2. Research method

The structural and electrical characteristics of Nd-adsorption silicene nanoribbons are investigated using the DFT method. All calculations are finished using the VASP software package. The many-body exchange and correlation energies, which are obtained from electron-electron Coulomb interactions, are calculated using the Perdew-Burke-Ernzerhof (PBE) functional. Additionally, the intrinsic electron-ion interactions are characterized by the projector-augmented wave (PAW) pseudopotentials. This set of plane waves has a 400 eV kinetic energy cutoff, which is more than enough to analyze Bloch wave functions and electronic energy spectra. The DFT method is used to look into the structural and electrical characteristics of Nd-adsorption silicene nanoribbons. The VASP software suite is used to conduct all of the calculations. The Perdew-Burke-Ernzerhof (PBE) functional is used to determine the energies for the many-body exchange and correlation processes, which are derived from electron-electron Coulomb interactions. The projector-augmented wave (PAW) pseudopotentials can also be used to represent the fundamental electron-ion interactions.

$$\Delta E = E_{\text{Nd/ASiNRs}} - E_{\text{Nd}} - E_{\text{ASiNRs}} \quad (1)$$

where E_{Nd} , E_{ASiNRs} , and $E_{\text{Nd/ASiNRs}}$ are the total energy of Nd atom, ASiNRs, and Nd adatom adsorbed on ASiNRs.

3. Results and analysis

3.1. Structural properties

It is shown how to construct a survey model using a monolayer ASiNRs model with N of 6 (See Figure 1). The model uses Nd as the study metal, and its basic structure consists of 12 C and 4 H atoms. We set up four Nd adsorption models based on ASiNRs: top, valley, bridge and hollow (see **Figure 1**).

After loading the code and running on the VASP program with 4 files INCAR, KPOINTS, POSCAR, and CONTCAR the binding energy is calculated according to formula (1) giving the results in **Table 1**.

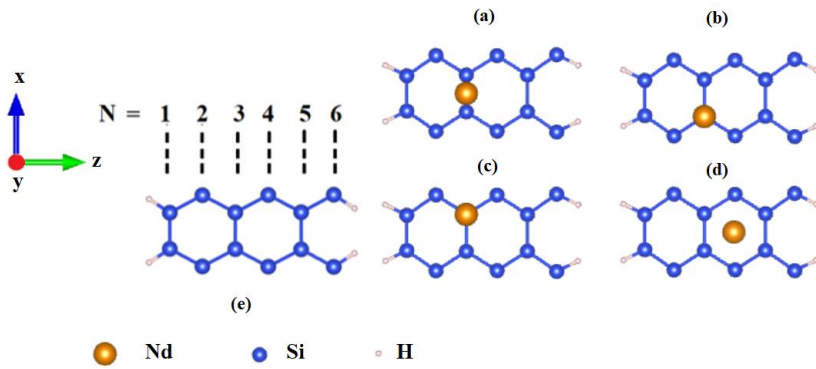


Figure 1. Structures POSCAR (a) Bridge, (b) Valley, (c) Top, (d) Hollow, (e) Pristine.

Table 1. Table of results for calculating and structuring states of the 4 positions.

V_j tri	Valley	Top	Bridge	Hollow	Pristine
E_{ASiNRs} (eV)	-69.56	-69.56	-69.56	-69.56	-69.56
E_{Nd} (eV)	-2.61	-2.94	-2.60	-2.48	x
$E_{Nd/AsiNRs}$ (eV)	-74.26	-74.27	-74.76	-74.56	x
ΔE (eV)	-2.09	-1.76	-2.60	-2.52	x
Buckl (Å)	0.40	0.40	0.69	0.38	0.44
Hight (Å)	7.35	7.75	4.70	4.13	0.00
Deg (deg)	117 ⁰⁰⁶ '	117 ⁰⁰⁶	115 ⁰⁵³ '	117 ⁰²⁷ '	116 ⁰²⁸ '
Mag (μB)	3.86	3.86	4.68	4.28	0.00
E_g (eV)	0	0	0	0	0,33
Structure states	H	H	H	H	H

Based on **Table 1**, we see through the calculation results that we have obtained values such as: formation energy of metal E_{Nd} , formation energy of substrate SiH, energy of formation of substrate (E_{ASiNRs}) ASiNRs. Formation of the absorption system including ASiNRs and Nd ($E_{Nd/ASiNRs}$). Besides, there are calculation results of buckling, height of metal atom Nd on the surface compared to pristine, bond angle between 3 nearest atoms Si-Si-Si and moment value. From Mag, the structural states consider the stability of the bonds after adsorption together between the Nd metal and the pristine substrate surface ASiNRs. Through **Table 1**, we look at the initial substrate ASiNRs as a basis so that after metal absorption we have new results, through which we can compare all the similar and different properties. Specifically, in the case of pristine substrate ASiNRs with

configuration N=6 consisting of 12 Si atoms and 4 H atoms. Originally a semiconducting compound, non-magnetic, with formation energy -69,56 eV, has a buckling of 0.44 Å, bond-angle between 3 Si atoms is 116029° deg, band gap 0.33 eV.

After calculating, we immediately commented on the results and found that: the positions (top, valley, hollow, bridge) all have stable configuration (H - High), equally stable. However, when we consider and compare the cases there are differences in detail, through which we can see which position gives the best result we expect. According to the results of **Table 1**, the Bridge position has the lowest value of absorbed energy, which can be understood as the most stable, with the strongest magnetic moment of 4.68 μ_B and relatively high buckling of 0.69 Å; The Si-Si-Si bond angle at this time 115028° is also close to the pristine case where this angle has a value of 116027°. The above factors show that the Bridge position is considered an effective position. Most effective compared to the remaining sites when allowing Nd to absorb ASiNRs.

3.2. Electronic properties

When considering the energy band structure of the ASiNRs substrates, we obtained the results as shown in **Figure 2** below.

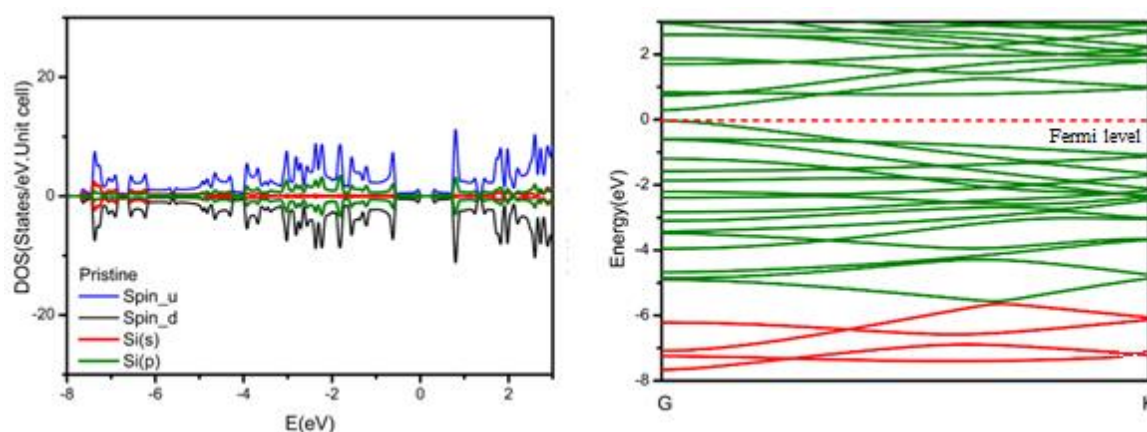


Figure 2 (a). Pristine DOS structure, (b) Pristine band structure.

According to the energy band structure in **Figure 2** drawn from the file vasprun.xml of ASiNRs material on Origin software, when choosing the Fermi energy level equal to 0 eV, through the calculation results, we can see the characteristic strongly active electron orbitals of ASiNRs here are Si (4s) in red and Si (3p) in green; The band gap energy value of pristine is $E_g = 0.33$ eV. At that time, the Si (4s) orbitals usually have high energy and are located deep at the bottom of the valence band (from -5eV to -8eV). The Si (3p) orbital electrons are concentrated in both the conduction band (above the fermi level) and the valence band (below the fermi level). The band gap E_g of the studied material is formed from these orbital electrons. According to **Figure 4**, the DOS state density of the obtained ASiNRs shows that the Si (4s) orbital electron energies are relatively strong compared to Si (3p), the energy value of Si (4s) level is about 5 (unit) and is strongest in the -3eV to -1eV region. The electronic energy of Si (3p) is relatively small, mainly at the bottom of the valence band (from -7.5eV to -6.5eV).

Based on **Figure 3**, and **Figure 4**, we represent the electron orbitals with corresponding colored lines Si (4s)_Brown; Si (3p)_Dark green; Si (3d)_Light green; Nd(s)_Orange; Nd(p)_Pink; Nd(d)_Ink blue; Nd(f)_Red. Considering **Figure 3**, the electronic band structures of the Nd metal absorption cases on the ASiNRs semiconductor background at different positions are different top, valley, bridge and hollow. They have in common that after absorbing the Nd atom the electronic orbitals near the Fermi level for pristine ASiNRs that are semiconductors now have overlap between the valence and conduction bands by the electronic interactions of the participation of the orbital electrons joined by Nd, that is, red Nd(d) in the vicinity of the Fermi level from -0.5eV to 0.5eV and Nd(f) in the conduction band from 0.5eV to 2eV covering for all four sites studied. Especially with **Figure 3**, we see the participation of Si (d) electron orbitals in the conduction band when absorption of Nd/ASiNRs occurs, but when in the pristine state, this orbital electron does not participate in the structure. Its characteristic Band region architecture.

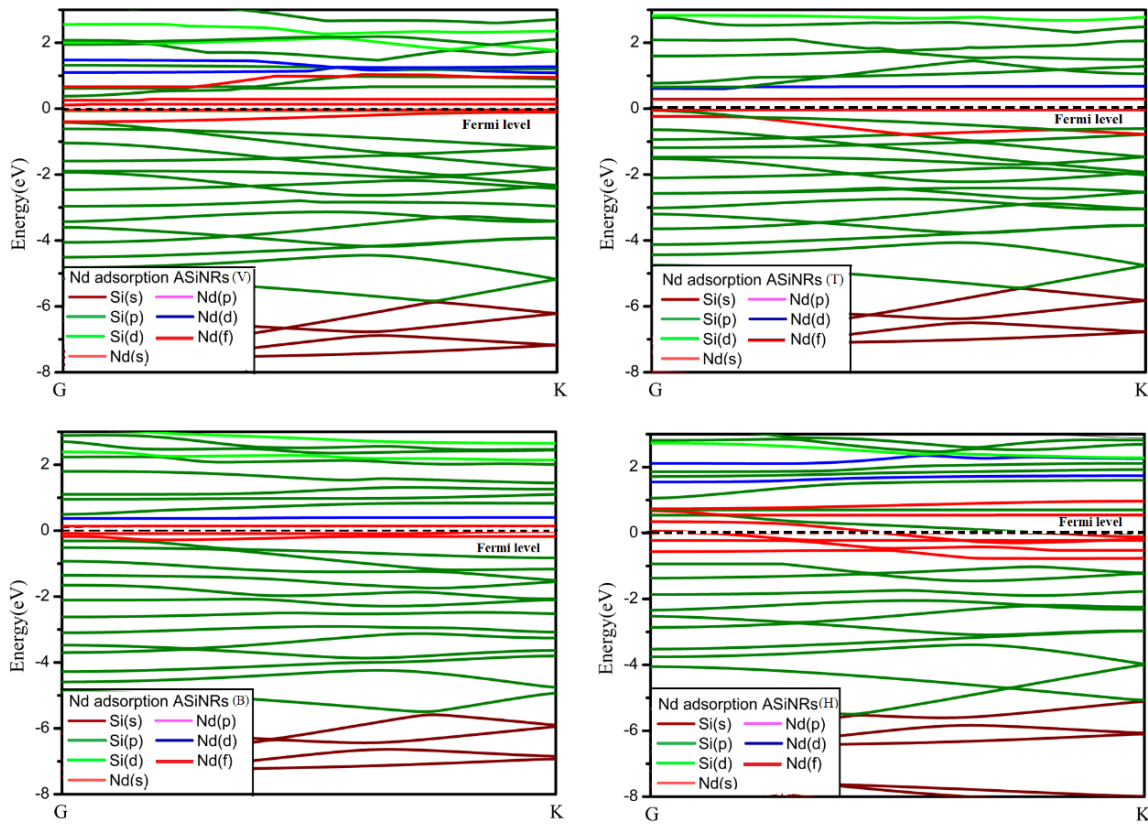


Figure 3. BAND structures of 4 positions Valley, Top, Bridge, and Hollow.

In **Figure 4**, the DOS state density of the top, valley, bridge and hollow cases we find that they have similarities, similar to that considered on the band in the energy region in **Figure 3**. However, the participation of Nd(f) electron orbitals in each different case will have different strengths and weaknesses. For the V-Valley position, the Nd(f) electron orbitals mainly appear in the conduction band with energies from -0.2eV to 1eV and with a strength of about 40 (units). The Nd(f) electron orbital T-Top site is active mainly in the vicinity of Fermi from -0.1eV to 0.8eV and the magnitude is relatively large, around 60 (states/eV). For the case at the B-

Bridge position, the Nd(f) orbital electrons are concentrated in the conduction band, it operates from -0.3eV to 0.5eV and the intensity is also large, the highest is about ~ 45 (states/eV)). Particularly for the case at the hollow position, the orbital electrons operate in a very wide range from the top of the valence band to the bottom of the conduction band, the energy is in the range of -1eV to 1eV and the intensity is also relatively uniform between the electrons orbit, amplitude is about ~ 30 (states/eV).

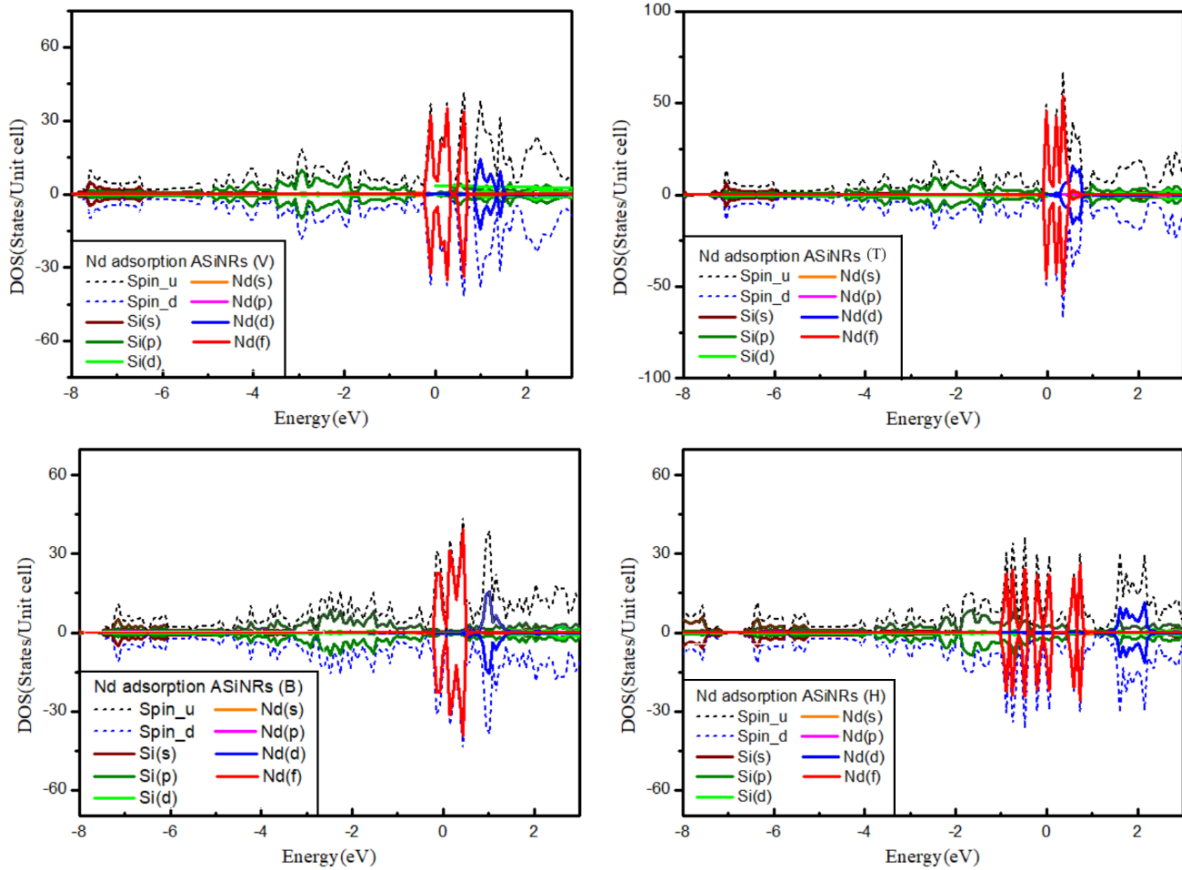


Figure 4. DOS structures of 4 positions Valley, Top, Bridge, and Hollow.

By examining the CHGCAR file of Nd adsorption cases on the background of ASiNRs at 4 different locations top, valley, hollow and bridge, we have the results as shown in **Figure 5**. Considering at 4 different positions from the results of reviewing the structural state of the CONTCAR file (drawn on VESTA software) and looking at the images of the model of the electronic orbitals in the cases shown. When we choose, the charge concentration is shown on the color axis from 0 to 0.07 e/A³ with the color range from B-G-R and plotting the composite files on VESTA we found. To consider the charge displacement during absorption between the substrate and the metal, we use the following calculation formula:

$$\Delta\rho = \rho_{Nd/ASiNRs} - \rho_{ASiNRs} - \rho_{Nd} \quad (2)$$

where, $\rho_{Nd/ASiNRs}$ is the charge density of the system after doping; ρ_{ASiNRs} is the charge density of the substrate before doping; ρ_{Nd} is the charge density of the doped metal component.

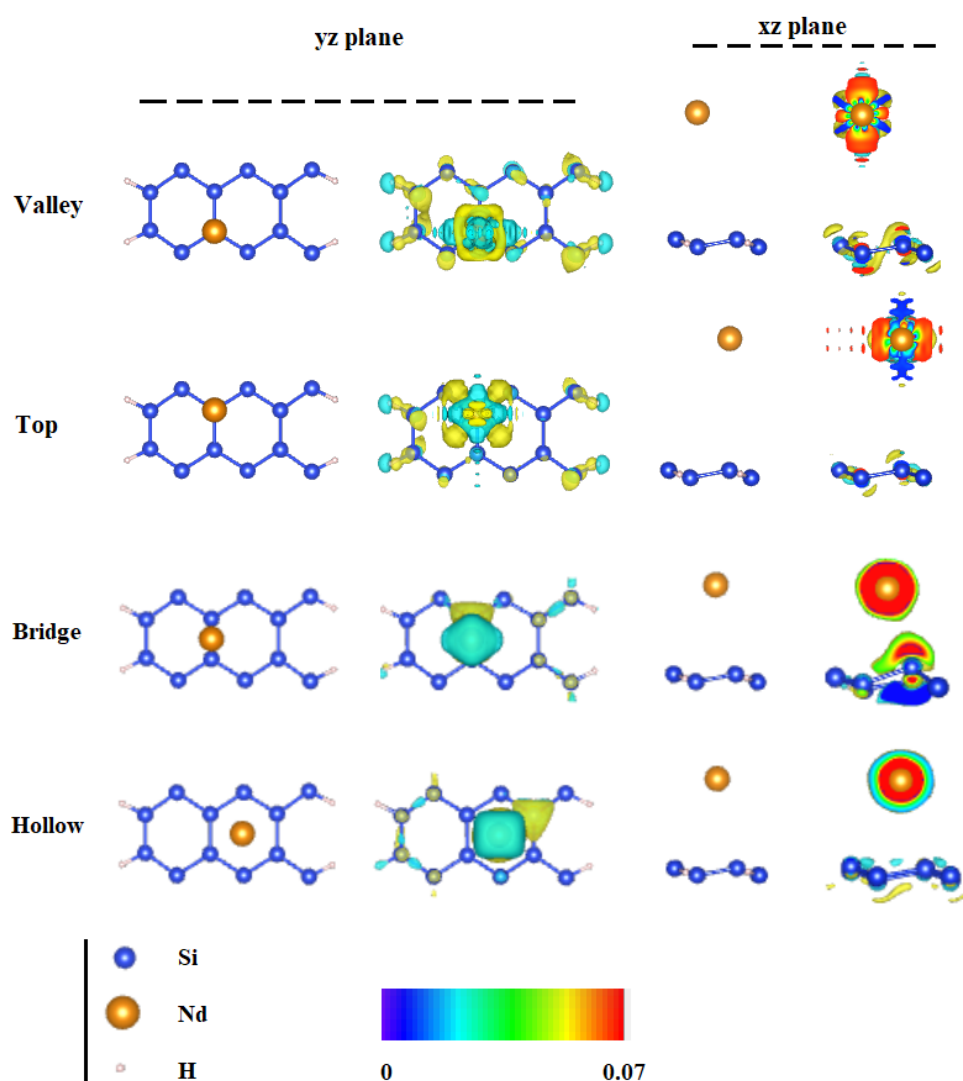


Figure 5. CONTCAR files and CHARCAR files of 4 positions.

The electrons belonging to the Si atoms in the vicinity of the present Nd site tend to participate in more or less charge interactions, the donating and accepting charges of the electron regions are occurring from here, resulting in leads to electron displacement, creating valence band filling and conduction band electrons, ready to move in the presence of an interacting external electric field (which is the general case of the 4 Nd-doped states that all new compounds are metallic, band gap $E_g = 0$).

Looking at the Bridge case of Figure 5, the electrons orbiting around the Nd atom in the Nd(f) orbital state have a very strong charge, which tends to pull the Nd atom towards the pristine substrate ASiNRs. At the same time, the participation of Si(d) electrons leads to more warping than in other cases, specifically here the degree of Buckl is 0.69\AA compared to Buckl of 0.4\AA (for Top case). , Valley), and 0.38\AA (Bridge case).

Table 2. OUTCAR file results, charge displacement of ASiNRs.

total charge				
# of ion	s	p	d	tot
1	1.051	1.486	0.116	2.652
2	1.051	1.486	0.116	2.653
3	1.057	1.426	0.098	2.581
4	1.057	1.428	0.098	2.582
5	1.059	1.411	0.096	2.566
6	1.059	1.412	0.096	2.567
7	1.059	1.412	0.096	2.567
8	1.059	1.412	0.096	2.567
9	1.057	1.428	0.098	2.582
10	1.057	1.426	0.098	2.581
11	1.050	1.486	0.116	2.652
12	1.050	1.485	0.116	2.651
13	0.194	0.001	0.000	0.196
14	0.194	0.001	0.000	0.196
15	0.194	0.001	0.000	0.196
16	0.194	0.001	0.000	0.195
tot	13.44	17.30	1.24	31.98

We proceed to consider the electronic transition from Nd atom to ASiNRs and vice versa through specific orbitals by reviewing the calculation results on HPCC with VASP software according to DFT theory.

From the calculation results of the OUTCAR file of the pristine configuration of pristine ASiNRs consisting of 12 Si atoms and 4 H atoms (**Table 2**), it shows that Si atoms have the participation of Si(s) electron orbitals, Si(p) and Si(d). However, for the Si(d) orbital, the charge density is so small that it can be ignored, compared to other orbitals Si(s) and Si(p) and this is clearly shown in **Figure 4**, which shows the structure of the orbitals electronic band structure of ASiNRs. Particularly for H atoms in the order numbers from 13 to 16, the electron orbitals H(1s) also have a very low electron density of about $0.194 \text{ e}/\text{\AA}^3$, the lower H(2p) and are also considered as insignificant, can be ignored.

Table 3. OUTCAR file results, charge displacement Nd/ASiNRs.

total charge					
# of ion	s	p	d	f	tot
1	1.044	1.363	0.110	0.017	2.533
2	1.043	1.369	0.111	0.017	2.540
3	1.053	1.270	0.090	0.011	2.424
4	1.051	1.329	0.090	0.011	2.481
5	1.047	1.272	0.084	0.009	2.412
6	1.058	1.250	0.089	0.011	2.408
7	1.054	1.251	0.087	0.011	2.403
8	1.049	1.278	0.086	0.011	2.424
9	1.048	1.307	0.087	0.011	2.453
10	1.046	1.310	0.088	0.011	2.456
11	1.041	1.360	0.109	0.016	2.527
12	1.044	1.371	0.109	0.017	2.542
13	0.195	0.001	0.000	0.000	0.196
14	0.196	0.001	0.000	0.000	0.198
15	0.194	0.001	0.000	0.000	0.195
16	0.195	0.001	0.000	0.000	0.196
17	1.922	5.461	0.036	8.422	15.840
tot	15.28	21.20	1.18	8.58	46.23

Based on the results of Table 3, it is shown that the Nd atom has a very large change in charge density of the Nd(f) orbital when participating in absorption on the surface of ASiNRs, whose charge value varies much from 4.874 into 8.58 e/Å³. Besides, the participation of Nd(p) also contributes to the formation of new compounds, contributing very important orbital charges. In this case, they accept electrons from Si(3p) to switch to Nd(p), so its charge density also increases from 5,399 to 5.461 e/Å³.

4. Conclusion

In this project, we initially learn about VASP and study some properties and configurations of silicene nanoribbon when doping with Nd, thereby proposing a model to create new electronic materials for the future, applying used in materials science and engineering science. There are 4 configurations studied: top, valley, bridge and hollow configuration. The original configuration of SiNRs is a semiconductor with a band gap of 0.33eV. After Nd doping, the top, valley, bridge and hollow configurations all become semi-metallic with Fermi-level cutoff energies, going from the conduction band to the valence band, but without band gap.

The contribution of Si states in the pristine configuration ASiNRs lies in the valence band middle and top for Si(s) and conduction band bottom for Si(p). Between them exists a band gap E_g that is characteristic of a semiconductor. So when doping Nd into ASiNRs with 4 different configurations, the results show:

- All 4 configurations give the compound formed semiconducting, magnetic
- Particularly, the Bridge configuration gives the most satisfactory result that is the band gap $E_g=0$ with the stable structure being the lowest absorption energy, the participation of orbital electrons of Nd(f) and Nd(d) is also very powerful in shifting the charge from the valence band to the conduction band. As a result, the substrate ASiNRs turns to metal in the presence of Nd absorption. The characteristic magnetic moments of doped Nd/ASiNRs have relatively large values, which have the potential to be used to fabricate future devices such as spin motors, field-effect transistors.

Acknowledgements

This research used resources of the high-performance computer cluster (HPCC) at Thu Dau Mot University (TDMU), Binh Duong Province, Vietnam.

Author contribution

All work is done by Thanh Tung Nguyen.

Funding

This research is funded by Thu Dau Mot University, Binh Duong province, Vietnam.

Competing interests

The author declare no competing interests.

References

1. Boubekeur Lalmi, Hamid Oughaddou, Hanna Enriquez, Abdelkader Kara, Sébastien Vizzini et al, Epitaxial growth of a silicene sheet, Applied physics letters, 2010, 97 (22): 223109. <http://link.aip.org/link/doi/10.1063/1.3524215?ver=pdfcov>
2. Kyozauro Takeda and Kenji Shiraishi, Theoretical possibility of stage corrugation in Si and Ge analogs of graphite, Phys Rev B, Vol 50, 20, 1994, <https://doi.org/10.1103/PhysRevB.50.14916>
3. Takeda K and Shiraishi K, Theoretical possibility of stage corrugation in Si and Ge analogs of graphite, Phys. Rev. B. 50, 14916-22, 1994. <https://doi.org/10.1103/PhysRevB.50.14916>
4. Mathew J. Cherukara, Badri Narayanan, Henry Chan, Subramanian K.R.S. Sankaranarayanan, Silicene growth through island migration and coalescence, Nanoscale, 2017,9, 10186-10192, <https://doi.org/10.1039/C7NR03153J>
5. Cherukara M J, Narayanan B, Chan H, and Sankaranarayanan S K R S, Silicene growth through island migration and coalescence, Nanoscale. 9, 10186-92, 2017. <https://doi.org/10.1039/C7NR03153J>
6. Tang C, Oppenheim T, Tung V C and Martini A, Structure–stability relationships for graphene- wrapped fullerene-coated carbon nanotubes, Carbon. 61, 458–66, 2013. <http://dx.doi.org/10.1016/j.carbon.2013.04.103>
7. Sadeddine S et al., Compelling experimental evidence of a Dirac cone in the electronic structure of a 2D Silicon layer, Sci. Rep. 7, 44400, 2017. <https://doi.org/10.1038/srep44400>
8. Gogotsi Y and Anasori B, The rise of Mxenes, ACS Nano. 13, 84914, 2019. <https://doi.org/10.1021/acsnano.9b06394>
9. Lima M P, Fazzio A and Silva A J R da, Silicene-based FET for logical technology, IEEE Electron Device Lett. 39, 1258–61, 2018. <https://doi.org/10.1149/2162-8777/abd09a>
10. Aghaei S M, Monshi M M and Calizo I, A theoretical study of gas adsorption on silicene nanoribbons and its application in a highly sensitive molecule sensor, RSC Adv. 6, 94417–28, 2016. <https://doi.org/10.1039/C6RA21293J>
11. Galashev A Y and Ivanichkina K A, Silicene anodes for lithium – ion batteries on metal substrates, J. Electrochem. Soc. 167, 50510, 2020. <http://dx.doi.org/10.1149/1945-7111/ab717a>
12. Sadeddine S et al., Compelling experimental evidence of a Dirac cone in the electronic structure of a 2D Silicon layer, Sci. Rep. 7, 44400, 2017. <https://doi.org/10.1038/srep44400>
13. Liu C-C, Feng W, and Yao Y, Quantum spin Hall effect in silicene and two-dimensional germanium, Phys. Rev. Lett. 107, 76802, 2011. <https://doi.org/10.1103/PhysRevLett.107.076802>
14. Ni Z et al., Tunable band gap in silicene and germanene, Nano Lett. 12, 113, 2012. <https://doi.org/10.1021/nl203065e>
15. Jia T-T et al., Band gap on/off switching of silicene superlattice, J. Phys. Chem. C. 119, 20747, 2015. <https://doi.org/10.1021/acs.jpcc.5b06626>
16. Drummond N D, Zólyomi V and Fal'ko V I, Electrically tunable band gap in silicene, Phys. Rev. B. 85, 75423, 2012. <https://doi.org/10.1103/PhysRevB.85.075423>
17. Lin S-Y, Liu H-Y, Nguyen D K, Tran N T T, Pham H D, Chang S-L, Lin C-Y and Lin M-F, Stacking-configuration-enriched fundamental properties in bilayer silicenes, Silicene-Based Layer. Mater., 5–28, 2020. <https://doi.org/10.48550/arXiv.1912.10257>
18. Jia T-T et al., Band gap on/off switching of silicene superlattice, J. Phys. Chem. C. 119, 20747, 2015. <https://doi.org/10.1021/acs.jpcc.5b06626>
19. Drummond N D, Zólyomi V and Fal'ko V I, Electrically tunable band gap in silicene, Phys. Rev. B. 85, 75423, 2012. <https://doi.org/10.1103/PhysRevB.85.075423>
20. A. Fleurence, R. Friedlein, T. Ozaki, H. Kawai, Y. Wang, Y. YamadaTakamura, Phys. Rev. Lett. 13,685-690, 2013. <https://doi.org/10.1103/PhysRevLett.111.107004>
21. Mehdi Aghaei S, Torres I and Calizo I, Structural stability of functionalized silicene nanoribbons with normal, reconstructed, and hybrid edges, Nanomater., 5959162, 2016. <http://dx.doi.org/10.1155/2016/5959162>
22. Chuan M W, Wong K L, Hamzah A, Riyadi M A, Alias N E and Tan M L P, Electronic properties of silicene nanoribbons using tight-binding approach, International Symposium on Electronics and Smart Devices (ISESD), 1–4, 2019. <http://dx.doi.org/10.1109/ISESD.2019.8909598>
23. University of Basel, Corrugated Structure of 2D Material Silicene Precisely Measured, 2019. <https://doi.org/10.1073/pnas.1913489117>
24. Ghasemi N, Ahmadkhan Kordbacheh A and Berahman M, Electronic, magnetic and transport properties of zigzag silicene nanoribbon adsorbed with Cu atom: a first-principles calculation, J. Magn. Magn. Mater. 473, 306-11, 2019. <http://dx.doi.org/10.1016/j.jmmm.2018.10.059>
25. Xu L, Wang X-F, Zhou L and Yang Z-Y, Adsorption of Ti atoms on zigzag silicene nanoribbons: influence on electric, magnetic, and thermoelectric properties, J. Phys. D. Appl. Phys. 48, 215306, 2015.

26. Werbowy, S., Windholz, L. Studies of Landé gJ-factors of singly ionized neodymium isotopes (142, 143 and 145) at relatively small magnetic fields up to 334 G by collinear laser ion beam spectroscopy. *Eur. Phys. J. D* 71, 16 (2017). <https://doi.org/10.1140/epjd/e2016-70641-3>
27. (2009) neodymium. In: Manutchehr-Danai M. (eds) *Dictionary of Gems and Gemology*. Springer, Berlin, Heidelberg. https://doi.org/10.1007/978-3-540-72816-0_15124
28. Haynes, William M., ed. (2016). "Neodymium. Elements". *CRC Handbook of Chemistry and Physics* (97th ed.). CRC Press. p. 4.23. ISBN 9781498754293. <http://www.hbcponline.com/>
29. Andrej Szytula; Janusz Leciejewicz (8 March 1994). *Handbook of Crystal Structures and Magnetic Properties of Rare Earth Intermetallics*, CRC Press. p. 1. ISBN 978-0-8493-4261-5. <https://doi.org/10.1201/9780138719411>
30. Stamenov P. (2021) Magnetism of the Elements. In: Coey J.M.D., Parkin S.S. (eds) *Handbook of Magnetism and Magnetic Materials*. Springer, Cham. https://doi.org/10.1007/978-3-030-63210-6_15
31. Greenwood and Earnshaw, *Chemistry of the elements*, School of Chemistry University of Leeds, UK, Elsevier, pp. 1235–8, 2005. <https://www.elsevier.com/books/chemistry-of-the-elements/greenwood/978-0-7506-3365-9>
32. T.J.Zhang et al, Experimental study of electrical properties at the Nd-doped Si-SiO₂ interface, *Journal of Physics and Chemistry of Solids*, Volume 48, Issue 6, 1987, Pages 551-554, [https://doi.org/10.1016/0022-3697\(87\)90050-3](https://doi.org/10.1016/0022-3697(87)90050-3)